PLOS ONE

RESEARCH ARTICLE

Vibration responses characteristics of a *Ginkgo biloba* tree excited under harmonic excitation

Huan Lin*, Leihou Sun

Department of Intelligent Equipment, Changzhou College of Information Technology, Changzhou, Jiangsu, China

* huanlinphd@163.com

OPEN ACCESS

Citation: Lin H, Sun L (2021) Vibration responses characteristics of a *Ginkgo biloba* tree excited under harmonic excitation. PLoS ONE 16(8): e0256492. https://doi.org/10.1371/journal.pone.0256492

Editor: Richard Mankin, US Department of Agriculture, UNITED STATES

Received: April 17, 2021

Accepted: August 7, 2021

Published: August 20, 2021

Data Availability Statement: All relevant data are within the paper and its Supporting information files.

Funding: This work was supported by the Natural Science Research Project of Universities in Jiangsu Province [grant number 19KJB210007], Changzhou Applied Basic Research Program [grant number CJ20190023], Scientific Research Project of Changzhou College of Information Technology [grant number CXZK201804Q], Scientific Research Platform of Changzhou College of Information Technology [grant numbers PYPT201804G], High-

Abstract

The most effective method of the fruit harvesting is the mechanical harvest. The frequency spectrum of different testing positions on a *Ginkgo biloba* tree under the impact excitation was tested in the laboratory. The acceleration responses under the harmonic excitation were measured at the frequency of the peak and trough points in the frequency spectrum curves. Results of this research indicate that the frequency spectrum presented the consistency on the same branch but distinction among different branches. There was a correspondence between the frequency spectrum characteristics and the vibration responses. The vibration responses could be strengthened at the resonant frequency. Merely, the acceleration responses at low frequency were very weak. At higher frequency, the vibration responses were strong but presented different characteristics among different branches. The acceleration response on the trunk was always the weakest. On the same branch, the dynamic responses presented the similar characteristics and the acceleration amplitude increased gradually as the testing position was located away from the excitation point on the trunk. Among different branches, the strongest dynamic response appeared at different frequencies. Our results indicate that it was difficult to induce the strong vibration response of all the branches at the single frequency during the practical mechanical harvesting of fruits.

1. Introduction

At present, mechanical harvest is the most effective method for the fruit harvesting [1–3]. Mechanical harvesters usually use the shaking or vibratory methods, such as air shaking, trunk shaking, limb shaking and canopy shaking [4,5]. The basic principle of vibratory harvesting is to transmit vibration energy to fruiting branches and then convert the energy into the traction force on fruit-stems. Fruits removal will occur when the traction force exceeds the tensile force of fruit-stems [6–8].

Studies were carried out to improve the removal efficiency of fruits. Torregrosa et al [9] used trunk and hand-held shakers to harvest several varieties of oranges and mandarins. Results showed that the tractor shaker was more effective (72% detachment) than hand-held shakers (57% detachment). Tests and analyses reflected that excitation amplitude, frequency,

end Equipment Manufacturing Intelligent Technology Innovation Team of Changzhou College of Information Technology [grant number CCIT2021STIT010201], Funded Project for Excellent Teaching Team of Jiangsu Qinglan Project.

Competing interests: The authors have declared that no competing interests exist.

duration and position affected the removal efficiency and the damage of fruits [10–12]. Loghavi et al [13] found that shaking the limbs at 80 mm amplitude and 10 Hz frequency with 98.5% lime fruit detachment was the most suitable combination. Erdoğan et al [14] discovered that the inertia type limb shaker should be operated within the range of 40 mm amplitude and 15Hz frequency to obtain maximum fruit removal with minimum vibration and reactive force. Mateev et al [15] established a probabilistic model for describing the vibratory fruit removal under different specified harvesting conditions and then validated the model precision. Harvesting robots were also studied to conduct basic experiments of the individual fruit or a targeted group of fruit [16,17].

The vibration response and energy transmission efficiency of the fruit trees were also researched. Du et al [18] studied the dynamic response of UFO (upright fruiting offshoots) cherry trees under the forced vibrations, and found that when the limb was excited at the low end near the trunk, the acceleration response of wood reached the maximum in the middle portion of both the trunk (horizontal) and the offshoots (vertical) at their resonant frequencies. Du et al [19] studied the dynamic characteristics of dwarf Chinese hickory trees under impact excitation and found that the variation of the dynamic response along the testing tree was greatly related to the crotch angle and the branch chain configuration. He et al [20] also studied the energy transmission of excited and neighboring limbs using a mechanical shaker in the "Y" trellised cherry orchard. Results revealed that the majority of energy (approximately 85% at 14 Hz shaking) was transmitted to the excited limbs. The variation of the energy distribution along a limb excited at different positions brings the possibility of obtaining different fruit removal efficiencies. The energy equation to the crank slider and eccentric block vibratory harvesters was studied [21–23]. The vibration system including the dynamic damping coefficient, elastic coefficient and equivalent mass was established. The relationship between the excitation height and frequency was also concluded.

Tree generally grows into the branch-on-branch structure and the limb vibration induced by the external force is often unevenly distributed on different parts of the tree [24]. Therefore, a better understanding of the behavior and dynamic characteristics of plants under forced vibration would help in designing mechanical harvesters [25]. Castro-García, et al [26] tested the modal parameters of olive trees and found that they were determined by the mass distribution, stiffness, and morphology. A series of experimental modal analysis was performed by using the stepping sinusoidal excitation, one-position excitation and multi-position acceleration response method. The wide distributions of data were shown in the damping ratio, modal mass and modal stiffness of the blackcurrant branches [27]. Rodriguez et al [28] analyzed the case of an idealized sympodial tree to understand the multimodal dynamics of trees and to quantitatively explain the role of geometry on their dynamical characteristics. Rodriguez et al [29] studied the vibration modes of the tree and validated a previous analytical approach that predicted the organization of modal frequencies as a function of two allometry parameters. Moore et al [30] tested the natural frequency and damping ratio of trees, then pointed out that it might not be appropriate to treat branches as lumped masses rather than individual cantilevers attached to the main stem.

During the vibratory harvest, the traction force on fruit-stems has the positive correlation with the acceleration in spatial directions. Whereas, Du et al [30,31] only studied the axis parallel to the direction of excitation and the maximum acceleration, which couldn't completely reflect the response characteristics of trees. Although the spectral analysis method was the conventional method during the signal analysis, the frequency response characteristics between the anisotropic live trees and the isotropous metal components had no comparability. Therefore, the frequency spectrum characteristics and the corresponding vibration responses in spatial directions on a *Ginkgo biloba* tree were determined. The objective of the current work was

to find the relationship between the frequency spectrum characteristics and the vibration responses.

2. Materials and methods

2.1 Experimental materials and distribution of testing positions

There was distinction among the physical and kinetic characteristics of different *Ginkgo biloba* trees. By pre-experiment, we have discovered that the fundamental frequency of *Ginkgo biloba* tree was low and strong acceleration response couldn't be induced by the fundamental frequency [32]. In order to completely analyze the relationship between the frequency spectrum characteristics and the vibration responses of different branches, one specimen was selected for the experiments and analysis. A 4-year-old Chinese *Ginkgo biloba* tree was selected as the experimental specimen from Nanjing Forestry University (Nanjing, Jiangsu Province, China, 32.1˚N, 118.8˚E). As shown in Fig 1, it mainly consisted of a trunk A from A_0 to A_1, two first

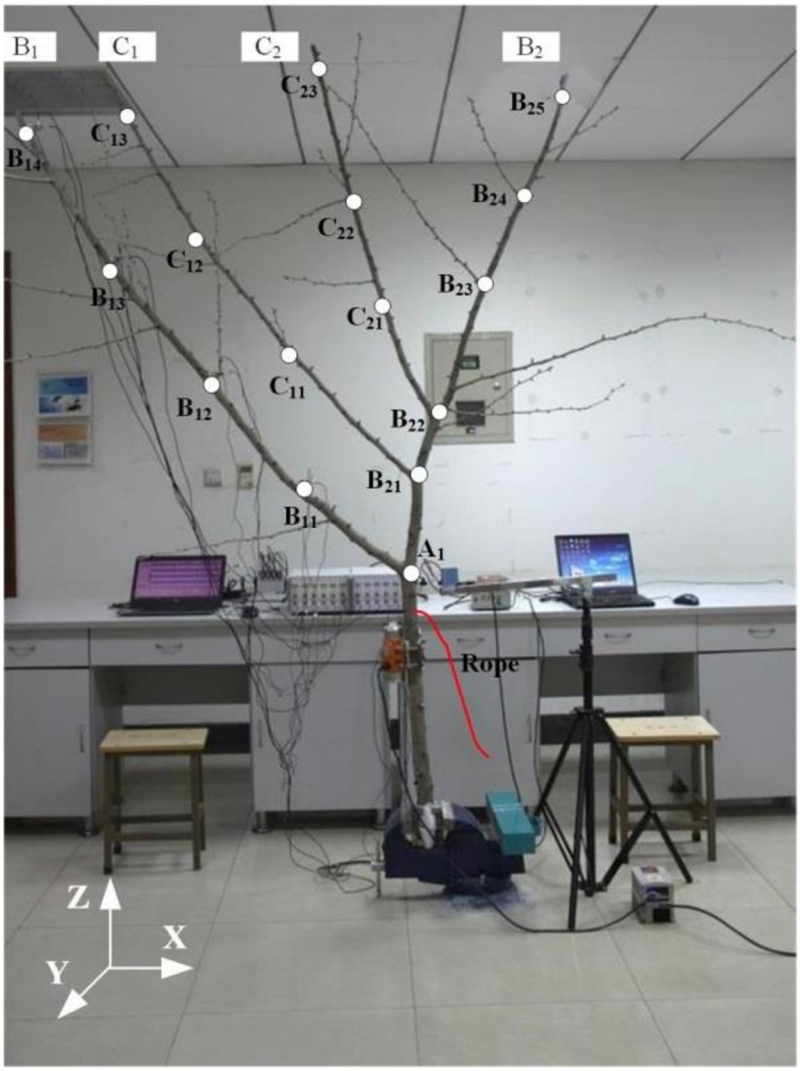

Fig 1. Diagram of tree specimen and data acquisition setup.

https://doi.org/10.1371/journal.pone.0256492.g001

Table 1. Dimension parameters of a *Ginkgo biloba* tree illustrated in Fig 1.

Branch rank		Testing position	Segment	Length/mm	Average diameter/mm
Trunk	A	A_1	A_0-A_1	900	50.1
First branch	B_1	B_{11}	B_{11}-A_1	445	27.2
		B_{12}	B_{12}-B_{11}	445	26.1
		B_{13}	B_{13}-B_{12}	445	22.0
		B_{14}	B_{14}-B_{13}	445	17.2
	B_2	B_{21}	B_{21}-A_1	292	35.5
		B_{22}	B_{22}-B_{21}	208	33.2
		B_{23}	B_{23}-B_{22}	343	20.8
		B_{24}	B_{24}-B_{23}	343	18.2
		B_{25}	B_{25}-B_{24}	343	13.9
Second branch	C_1	C_{11}	C_{11}-B_{21}	507	17.2
		C_{12}	C_{12}-C_{11}	507	14.3
		C_{13}	C_{13}-C_{12}	507	11.0
	C_2	C_{21}	C_{21}-B_{22}	393	19.8
		C_{22}	C_{22}-C_{21}	393	16.8
		C_{23}	C_{23}-C_{22}	393	14.5

https://doi.org/10.1371/journal.pone.0256492.t001

branches B_1, B_2 originating from the trunk and two second branches C_1, C_2 originating from branch B_2. All the branches were almost located in the same perpendicular plane.

The root and leaves were removed and the total mass of this tree specimen was 4.46 kg. During the experiment, the segment below position A_0 was fixed vertically using clamps to ground. Testing positions A_1, B_{21}, B_{22} were located at three crotch nodes and the other testing positions were averagely arranged according to the length of each branch. Every testing position was marked by a white circle. The major branch indexes and their geometric parameters were listed in Table 1. The experiments were conducted immediately after the tree specimen was delivered to the laboratory (March 16–18, 2020). The relative humidity of the laboratory was maintained at 60% and the temperature was controlled at 25˚C.

2.2 Method of testing the fundamental frequency and damping ratio

The fundamental frequency could be concluded by the pull-release test. As shown in Fig 2, testing equipment included a laser displacement sensor (OD-P85W20I0, SICK-Sensor Intelligence, Waldkirch, Germany), a 12V stabilized voltage supply (YU1220, Guangzhou Meanwell Electronic Product Co., Ltd. Guangzhou, China), a data acquisition device (HRU-420E, Shanghai Horizon Electronic Technology Co., Ltd. Shanghai, China), and a vibration testing and analysis software (HRsoft-DW V1.3, Shanghai Horizon Electronic Technology Co., Ltd. Shanghai, China).

A rope was tied on the trunk, then pulled and released to exert the step force on the tree specimen. The laser focused on a position 200 mm below the crotch node A_1. The fundamental frequency (ω_0, Hz) and damping ratio (ξ) could be calculated by the following equations, respectively:

$$\omega_0 = \frac{n}{t_{n+1} - t_1} \tag{1}$$

$$\xi = \frac{\ln\left(\frac{A_1}{A_{n+1}}\right)}{n \cdot 2\pi} \tag{2}$$

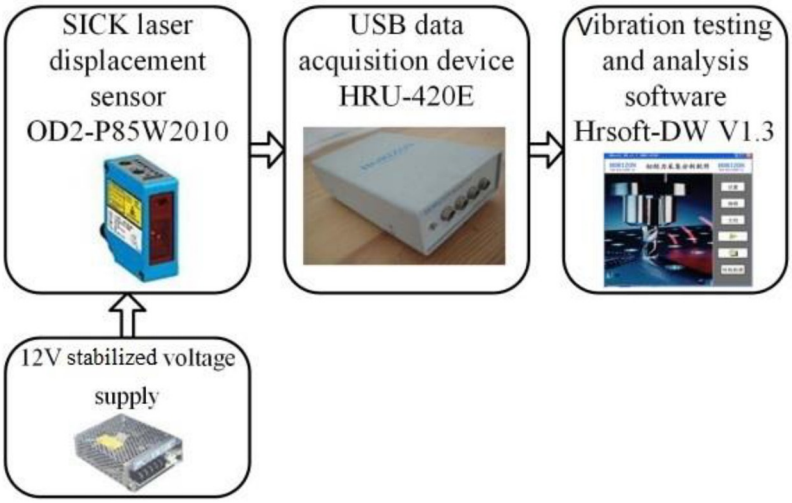

Fig 2. Equipment of testing fundamental frequency and damping ratio.

https://doi.org/10.1371/journal.pone.0256492.g002

Where, A_1 and A_{n+1} are the first and $n + 1$ peak values, t_1 and t_{n+1} are the corresponding time to reach these two peaks in the displacement attenuation curve (Fig 3).

2.3 Method of testing the frequency spectrum characteristics and vibration responses

The frequency spectrum characteristics of tree specimen were excited by the impacting force produced by an impact hammer (LC-02A, Jiangsu Sinocera Piezotronics Inc, Yangzhou, China). By computing the power spectrum with the recording and analyzing software (CRAS V7.1, The First Test Software Engineering, Co., Ltd, Nanjing, China), the frequency at the peak and trough points could be indicated.

As shown in Fig 4, the vibration response testing equipment consisted of a single-eccentric type harmonic excitation motor (Puta Vibrating Motor, Xin Jia Hong Technology Co., Ltd. Shenzhen, China), a frequency converter (JVFT-S5, Jinhui Instrumentation, Co., Ltd. Shenzhen, China), four triple-axis accelerometers (CA-YD-141, Jiangsu Sinocera Piezotronics Inc,

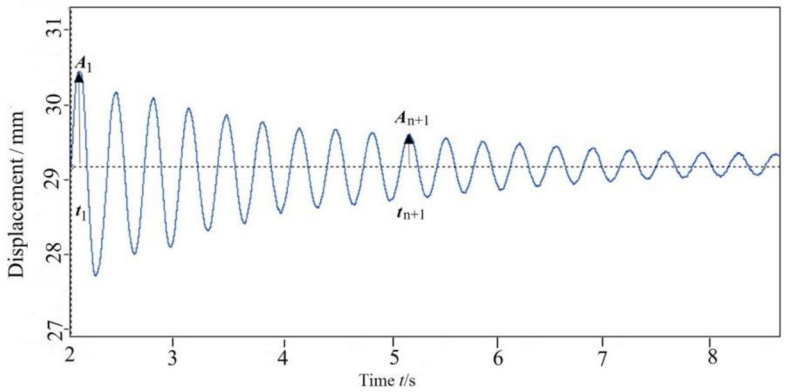

Fig 3. Displacement as a function of time under step force.

https://doi.org/10.1371/journal.pone.0256492.g003

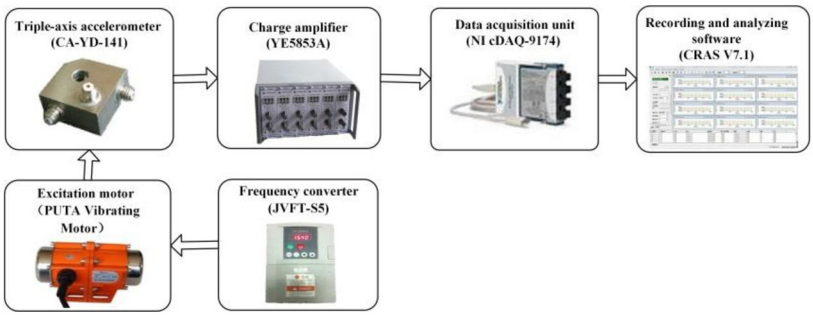

Fig 4. Schematic diagram of vibration response testing system.

https://doi.org/10.1371/journal.pone.0256492.g004

Yangzhou, China), two charge amplifiers (YE5853A, Jiangsu Sinocera Piezotronics Inc, Yangzhou, China), and three data acquisition units (NI cDAQ-9174, The National Instrument Co., Ltd, USA).

The excitation motor was fixed at a position with 400 mm below the crotch node A_1. The tree sample growing orientation was treated as the Z-direction. The X-direction was parallel to the connection line between the two central points of the motor and tree sample. As shown in Fig 1, Y-direction was vertical to these two directions. The triple-axis accelerometer could record the acceleration signals in three directions under the impact and harmonic excitations. In this paper, both the power spectrum amplitude and the acceleration response amplitude of each testing position were the resultant values of three directions.

Due to the limited number of accelerometers, only four testing positions could be tested in one test. During the experiment, when the treatments of four testing positions were completed, the accelerometers were moved to the next four testing positions until all positions were completed. The same treatment of each testing position was repeated three times and the test data was the average value of three measurements.

To describe the transmission characteristics of the dynamic response along the branches on the *Ginkgo biloba* tree, the dynamic acceleration transmission ratio (DATR) was defined using Eq (3).

$$k_{t(i)} = \frac{a_i}{a_0} \tag{3}$$

Where, $k_{t(i)}$ is the DATR of the testing position i, a_i is the acceleration of the testing position i, a_0 is the acceleration of the reference position. In this paper, the testing position A_1 was regarded as the reference position.

3. Results and discussion

3.1 Frequency spectrum characteristics

For the *Ginkgo biloba* tree illustrated in Fig 1, through pull-release test, the fundamental frequency was 2.50 Hz and damping ratio was 0.06 by calculation of Eqs (1) and (2) when n was selected as 10 in Fig 3.

By the impact excitation test, the acceleration curve as a function of time could be attained. The power spectrum curves could be computed by the frequency spectrum treatment. The first peak point occurred at 2.50 Hz for all the power spectrum curves (Figs 5a, 6a and 7a), in accordance with the fundamental frequency by pull-release test. Since the appropriate

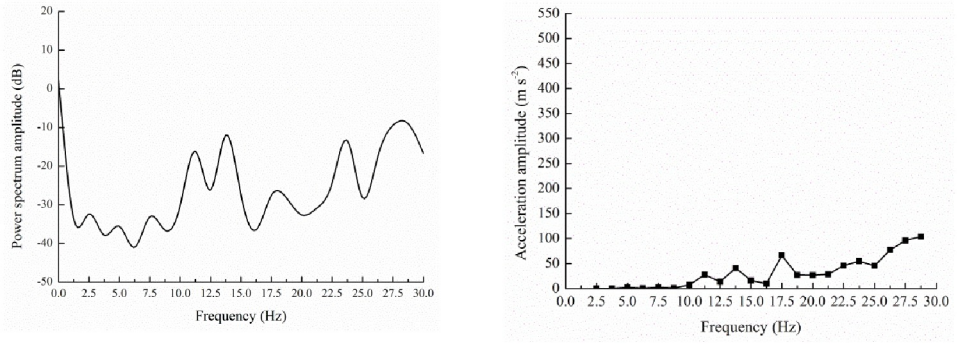

Fig 5. Power spectrum (a) and acceleration response (b) of testing position A_1.

https://doi.org/10.1371/journal.pone.0256492.g005

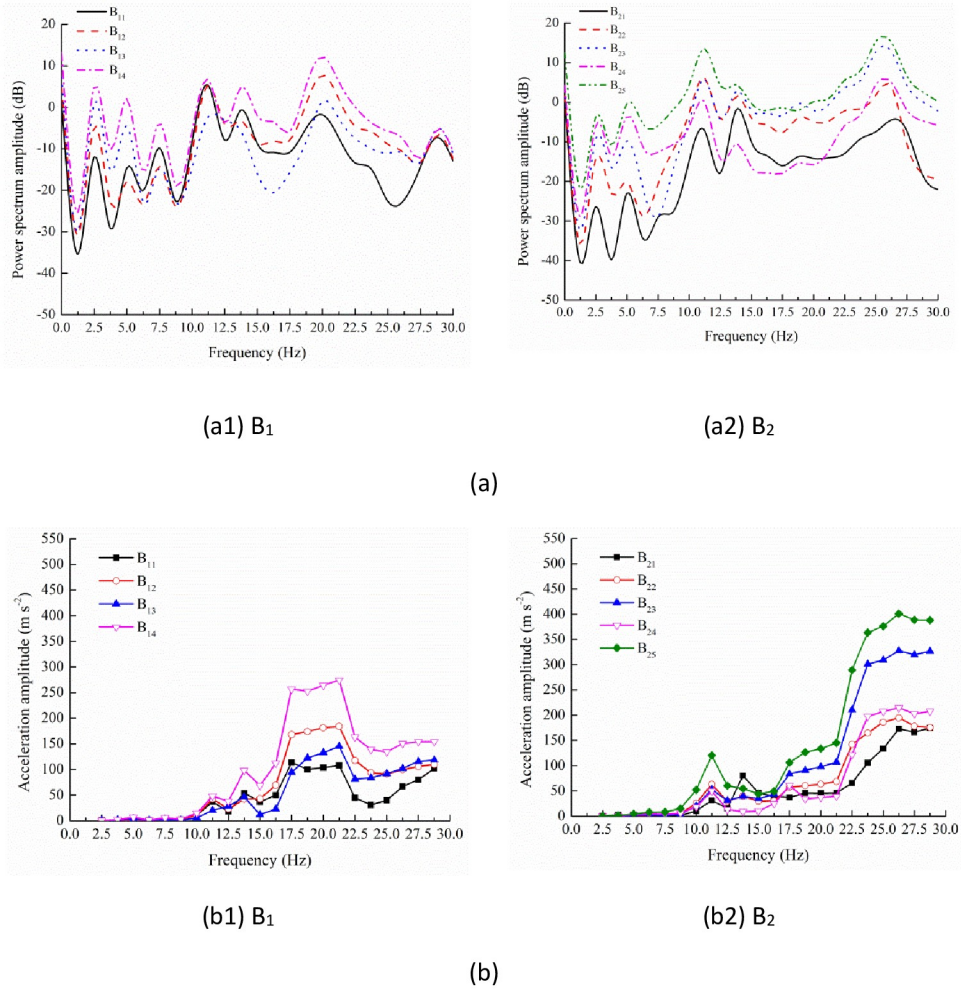

Fig 6. Power spectrum (a) and acceleration response (b) of testing positions on branches B_1 and B_2.

https://doi.org/10.1371/journal.pone.0256492.g006

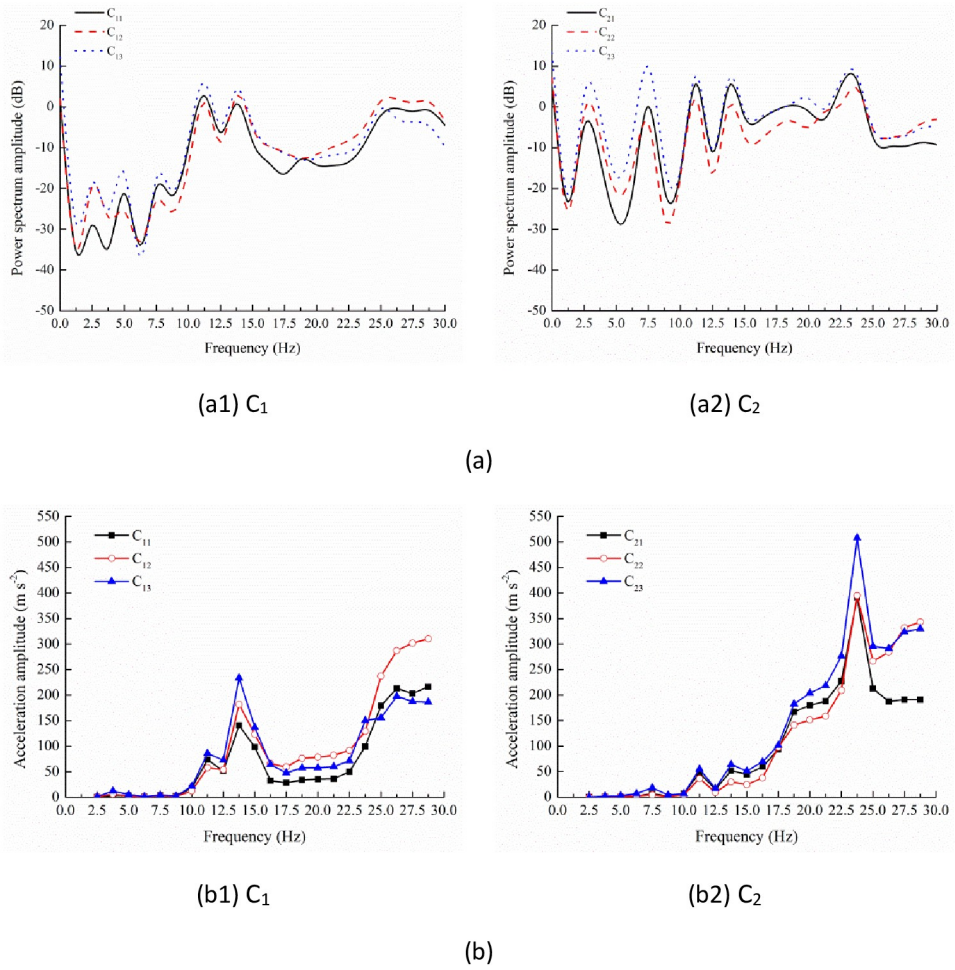

Fig 7. Power spectrum (a) and acceleration response (b) of testing positions on branches C_1 and C_2.

https://doi.org/10.1371/journal.pone.0256492.g007

excitation frequency was generally regarded as 10–30 Hz for the mechanical harvesting of fruits [33], the maximum analysis frequency was 30 Hz in the power spectrum.

At the testing position A_1, small peaks continuously appeared at 5.00 and 7.50 Hz when the frequency was lower than 10.00 Hz. Between 10.00 and 20.00 Hz, the primary peaks could be found at 11.25, 13.75 and 17.50 Hz. At higher frequency, there were two peaks at 23.75 and 28.75 Hz (Fig 5a).

On the same branch, the power spectrum curves of different testing positions presented similar characteristics (Figs 6a and 7a). Unlike the testing position A_1, 17.50 and 23.75 Hz weren't the resonant frequencies for branches B_1, B_2 and C_1. By contrast, on branch B_1, there was another peak at 20.00 Hz. On branch B_2, power spectrum curves also peaked at 26.25 Hz while there wasn't a peak at 7.50 Hz. On branch C_1, the lasting peak appeared at the frequency range 25.00–28.75 Hz. Nevertheless, the peaks only could be found at 7.50, 11.25, 13.75 and 23.75 Hz on branch C_2. The identification of frequency peaks on different branches was summarized in Table 2. Therefore, among the frequency spectrum curves of different branches, there was consistency when the frequency was lower than 15.00 Hz. Nevertheless, at higher frequency, the frequency spectrum curves presented the peak points at different frequencies.

Table 2. Resonant frequencies of tree specimen.

Branch rank	Frequency(Hz)									
	I	II	III	IV	V	VI	VII	VIII	IX	X
A_1	2.50	5.00	7.50	11.25	13.75	17.50		23.75		28.75
B_1	2.50	5.00	7.50	11.25	13.75		20.00			28.75
B_2	2.50	5.00		11.25	13.75				26.25	
C_1	2.50	5.00	7.50	11.25	13.75					25.00–28.75
C_2	2.50		7.50	11.25	13.75			23.75		

https://doi.org/10.1371/journal.pone.0256492.t002

3.2 Vibration responses under the harmonic excitation

In order to completely analyze the relationship between the frequency spectrum characteristics and the vibration responses, tree specimen was excited at the frequency where the apparent and slight peak and trough points occurred in the power spectrum curves (Table 2, Figs 5a, 6a and 7a).

Testing position A_1 located at the top of trunk and was the crotch node connecting branches B_1 and B_2. As shown in Fig 5b, the acceleration response was very weak at the I, II and III resonant frequency (Table 2). At the following resonant frequency of 11.25, 13.75 and 17.50 Hz, the acceleration amplitude reached the gradually increasing peaks 27.79, 40.71 and 66.65 m s^{-2}. Due to the existence of the trough point in the power spectrum curve (Fig 5a), the value was only 9.72 m s^{-2} at 16.25 Hz. At the VIII resonant frequency 23.75 Hz, the acceleration response reached the maximal value 54.71 m s^{-2}, which was smaller than the value at 17.50 Hz. When the excitation frequency was higher than 25.00 Hz, the acceleration amplitude increased obviously and attained the maximum 103.70 m s^{-2} at the X resonant frequency 28.75 Hz. It indicated that there was correspondence between the power spectrum characteristics and the acceleration responses.

For the branch B_1 (Fig 6b1), the vibration responses were weak when the frequency was lower than 10.00 Hz. Then, at the IV and V resonant frequency 11.25 and 13.75 Hz, the maximal acceleration amplitudes of four testing positions attained 47.75 and 98.41 m s^{-2}, respectively. At 17.50 Hz, the values increased sharply and then changed slightly with the frequency increasing to 21.25 Hz. At this frequency range, the average values reached 106.25, 177.00, 123.71 and 262.17 m s^{-2} for the testing positions B_{11}, B_{12}, B_{13} and B_{14}. This was probably due to the existence of the resonant frequency 20.00 Hz (Table 2). Between 21.25 Hz and 25.00 Hz, the acceleration amplitudes decreased promptly and presented the apparent trough range. When the frequency was higher than 25.00 Hz, the values increased gradually. Although there was another resonant frequency 28.75 Hz, the vibration responses weren't strengthened significantly again.

When the frequency was lower than 10.00 Hz, the vibration responses were also weak on branch B_2 (Fig 6b2). At the IV resonant frequency 11.25 Hz, the vibration responses were strengthened and the value reached 120.32 m s^{-2} at the testing position B_{25}. At the V resonant frequency 13.75 Hz, the acceleration amplitudes didn't increase observably except for the value at the testing position B_{21}. At the frequency range 15.00–21.25 Hz, the values presented increasing tendency but the increment was small. Nevertheless, when the frequency was higher than 21.25 Hz, the acceleration amplitudes of the five testing positions increased significantly and attained the maxima at the IX resonant frequency 26.25 Hz. The maxima were 2.76, 1.84, 2.06, 4.42 and 1.76 times larger than the values at 21.25 Hz, which was different from the characteristics on branch B_1. At higher frequency, all the acceleration amplitudes decreased slightly and the value of the testing position B_{25} was still the largest.

For the branch C_1 (Fig 7b1), the acceleration amplitudes of three testing positions were small at low frequency and increased to 58.03–86.29 m s^{-2} at the IV resonant frequency 11.25 Hz. At the V resonant frequency 13.75 Hz, the acceleration amplitudes reached 140.69, 181.89 and 233.63 m s^{-2} at the three testing positions C_{11}, C_{12} and C_{13}, which were much larger than the values at other testing positions. Then, the values decreased sharply and presented the trough range between 16.25 Hz and 22.50 Hz, which was in consistence with the power spectrum curve in Fig 7a1. However, when the frequency was higher than 22.50 Hz, the values presented significant increase. At 26.25 Hz, the peak values 213.30 and 197.93 m s^{-2} appeared at the testing positions C_{11} and C_{13}. At higher frequency, all the acceleration amplitudes didn't change a lot, which was similar to the values on branch B_2.

Similarly to the testing position A_1, branches B_1, B_2 and C_1, the vibration responses weren't strong until the frequency was higher than 10.00 Hz (Fig 7b2). The acceleration amplitudes attained small peaks at the IV and V resonant frequency 11.25 and 13.75 Hz. Then, the values increased gradually when the frequency was higher than 15.00 Hz. Especially at 18.75 Hz, the values increased by 79.08%, 44.75% and 79.71% than those at 17.50 Hz. At the VIII resonant frequency 23.75 Hz, the acceleration amplitudes reached 391.33, 395.15 and 508.15 m s^{-2}, which were larger than the value of 363.65 m s^{-2} at the testing position B_{25}. When the frequency was higher than 23.75 Hz, the acceleration amplitudes first decreased and then increased slightly. In addition, the values of the testing positions C_{22} and C_{23} were almost the same.

Consequently, there was a correspondence between the frequency spectrum characteristics and the vibration responses. Generally, the vibration responses were strengthened at the resonant frequency and attenuated at the frequency where the trough point appeared in the power spectrum curve. The vibration responses on the same branch presented the similar characteristics. Among different branches, the vibration responses were very weak when the frequency was lower than 10.00 Hz. At higher frequency, the vibration responses were strong but presented different characteristics.

3.3 Dynamic acceleration transmission characteristics

To reflect the transmission characteristics of the dynamic response, the DATRs of the testing positions on the tree specimen were calculated by Eq (3). The acceleration amplitudes under resonant frequencies 11.25, 13.75, 17.50, 20.00, 23.75 and 26.25 Hz were analyzed because they were identified as the most effective bands of excitation (Table 3).

On branch B_1, most of the DATRs were larger than 1.00, which reflected that the dynamic response was mainly enhanced on this branch. At 20.00 Hz, the values of the four testing positions reached the maxima 3.85, 6.76, 4.94 and 9.84. At the same frequency, the maximal DATR

Table 3. Obtained dynamic acceleration transmission ratio of different testing positions at resonant frequency.

Frequency/Hz	Testing position															
	A_1	B_{11}	B_{12}	B_{13}	B_{14}	B_{21}	B_{22}	B_{23}	B_{24}	B_{25}	C_{11}	C_{12}	C_{13}	C_{21}	C_{22}	C_{23}
11.25	1.00	1.33	1.53	0.73	1.72	1.13	2.28	1.90	1.78	4.33	2.65	2.09	3.10	1.70	1.32	1.98
13.75	1.00	1.33	1.03	1.13	2.42	1.97	0.98	0.97	0.22	1.34	3.46	4.47	5.74	1.27	0.73	1.57
17.50	1.00	1.70	2.52	1.42	3.86	0.56	0.86	1.25	0.92	1.59	0.42	0.89	0.72	1.40	1.47	1.52
20.00	1.00	3.85	6.76	4.94	9.84	1.69	2.36	3.64	1.39	4.98	1.32	2.92	2.15	6.70	5.63	7.59
23.75	1.00	0.56	1.71	1.53	2.54	1.93	3.01	5.51	3.61	6.65	1.81	2.36	2.75	7.15	7.22	9.29
26.25	1.00	0.87	1.29	1.32	1.95	2.24	2.52	4.24	2.78	5.19	2.76	3.72	2.56	2.42	3.68	3.77

https://doi.org/10.1371/journal.pone.0256492.t003

always occurred at the testing position B_{14} which was located furthest away from the excitation point. Meanwhile, the minimum of the testing position B_{14} also reached 1.72. Therefore, the dynamic response was always the strongest on the top of branch B_1.

On branch B_2, in total, there were six DATRs smaller than 1.00 at 13.75 and 17.50 Hz. As the frequency increased, the value of the testing position B_{21} attained the maximum 2.24 at 26.25 Hz. Whereas, the values of the other four testing positions attained the maxima 3.01, 5.51, 3.61 and 6.65 at 23.75 Hz. At the same frequency, among the five testing positions, all the maximal DATRs occurred at the testing position B_{25} except for 1.97 of the testing position B_{21} at 13.75 Hz.

For the three testing positions on branch C_1, the DATRs were only 0.42, 0.8 and 0.72 at 17.50 Hz. At the same time, the value of the junction point B_{21} was also smaller than 1.00. This exhibited that the dynamic response was attenuated when it was transmitted from the testing position A_1 to the testing position B_{21} and branch C_1. The maximal DATRs 3.46, 4.47 and 5.74 occurred at 13.75 Hz for the three testing positions C_{11}, C_{12} and C_{13}. At 11.25, 13.75 and 23.75 Hz, the maximum among the three testing positions occurred at the testing position C_{13}. By contrast, the maximum was found at the testing position C_{12} when the frequency was 17.50, 20.00 and 26.25 Hz.

For branch C_2, the only one DATR smaller than 1.00 occurred at the testing position C_{22} when the frequency was 13.75 Hz. Meanwhile, at the junction points B_{21} and B_{22}, the values were 1.97 and 0.98. This reflected that the dynamic response wasn't always enhanced during the process of transmission. As the frequency increased, the DATRs of the three testing positions attained the maxima 7.15, 7.22 and 9.29 at 23.75 Hz. The maxima were much greater than the values on other branches except for 9.84 of the testing position B_{14} at 20.00 Hz. Similarly to branch B_1, at the same frequency, the maximal DATR appeared at the testing position on the top of branch.

The transmission characteristics of the dynamic response were affected by the branch rank and the excitation frequency. Due to the distinction in the frequency spectrum, the strongest dynamic response of different branches appeared at different frequencies. Generally, at the same frequency, the strongest dynamic response could be tested at the testing position which was located furthest away from the excitation position.

4. Conclusions

Test with the impact excitation and pull-release test revealed the same fundamental frequency 2.50 Hz for the tree specimen. On the same branch, the frequency spectrum exhibited the similar characteristics. Among the frequency spectrum of different branches, there was consistency when the frequency was lower than 15.00 Hz but distinction at higher frequency.

Generally, the vibration responses were consistent with the frequency spectrum characteristics. The vibration response induced by the single-eccentric type harmonic excitation could be strengthened at the resonant frequency. Merely, the acceleration responses at low frequency were very weak. At higher frequency, the vibration responses were strong but presented different characteristics among different branches. The acceleration amplitude on the trunk was always the smallest.

On the same branch, the dynamic responses of the testing positions presented the similar characteristics. Generally, the acceleration amplitude increased gradually as the testing position was located away from the excitation point. Comparing different branches, the strongest dynamic response appeared at different frequencies. It indicated that in the practical mechanical harvesting of fruits, it was difficult to induce the strong vibration response of all the branches at the single frequency.

The morphology of trees mainly contains monopodial branching and sympodial branching. The *Ginkgo biloba* tree with two levels of branch was representative. In future research, trees with other shapes could be tested to verify if the results of this study were universal.

Supporting information

S1 Data.
(DOCX)

Author Contributions

Data curation: Huan Lin, Leihou Sun.

Formal analysis: Huan Lin.

Funding acquisition: Huan Lin.

Investigation: Leihou Sun.

Writing – original draft: Huan Lin.

Writing – review & editing: Huan Lin, Leihou Sun.

References

1. Peterson D L. Harvest mechanization progress and prospects for fresh market quality deciduous tree fruits. HortTech,2005, 15(1): 72–75.
2. Chen D, Du X Q, Wang S M, Zhang Q. Mechanism of vibratory fruit harvest and review of current advance. Transactions of the CSAE, 2011, 27(8): 195–200.
3. Wang C, Xu L Y, Zhou H P, Cui Y M, Cui H. Development and experiment of eccentric-type vibratory harvester for forest-fruits. Transactions of the CSAE, 2012, 28(16): 10–16.
4. Sanders K F. Orange harvesting systems review. Biosystems Engineering, 2005, 90(2): 115–125.
5. Adrian P A., Fridley R B. Dynamics and design criteria of inertia-type tree shakers. Transactions of the ASAE, 1965, 8(1): 12–14.
6. Markwardt E D, Guest R W, Cain J C, LaBelle R L. Mechanical cherry harvesting. Transactions of the ASAE, 1964, 7(1): 70–74.
7. Cooke J R, Rand R H. Vibratory fruit harvesting: A linear theory of fruit-stem dynamics. Journal of Agricultural Engineering Research, 1969, 14(3): 195–209.
8. Torregrosa A, Albert F, Aleixos N, Ortiz C, Blasco J. Analysis of the detachment of citrus fruits by vibration using artificial vision. Biosystems Engineering, 2014, 119(3): 1–12.
9. Torregrosa A, Ortí E, Martín B, Gil J, Ortiz C. Mechanical harvesting of oranges and mandarins in Spain. Biosystems Engineering, 2009, 104(1): 18–24.
10. Wang Y C, Chen H T, Lin Q. Optimization of parameters of blackcurrant harvesting mechanism. Transactions of the CSAE, 2009, 25(3): 79–83.
11. Zhou J F, He L, Zhang Q, Du X Q, Chen D, Karkee M. Evaluation of the influence of shaking frequency and duration in mechanical harvest of sweet cherry. Applied Engineering in Agriculture, 2013, 29(5): 607–612.
12. Zhou J F, He L, Zhang Q, Karkee M. Effect of excitation position of a handheld shaker on fruit removal efficiency and damage in mechanical harvesting of sweet cherry. Biosystems Engineering, 2014, 125 (9): 36–44.
13. Loghavi M, Mohseni S H. The effects of shaking frequency and amplitude on detachment of lime fruit. Iran Agricultural Research, 2006, 25(1): 27–38.
14. Erdoğan D, Güner M, Dursun E, Gezer İ. Mechanical harvesting of apricots. Biosystems Engineering, 2003, 85(1): 19–28.
15. Mateev L, Kostadinov G. Probabilistic model of fruit removal during vibratory morello harvesting. Biosystems Engineering, 2004, 87(4): 425–435.

16. Muscato G, Prestifilippo M, Abbate N, Rizzuto I. A prototype of an orange picking robot: Past history, the new robot and experimental results. Industrial Robot: An International Journal, 2005, 32(2): 128–138.

17. Tanigaki K, Fujiura T, Akase A, Imagawa J. Cherry-harvesting robot. Computers and Electronics in Agriculture, 2008, 63(1): 65–72.

18. Du X Q, Chen D, Zhang Q, Scharf P A, Whiting M D. Response of UFO (upright fruiting offshoots) on cherry trees to mechanical harvest by dynamic vibratory excitation. Transactions of the ASABE,2013, 56(2): 345–354.

19. Du X Q, Wu C Y, He L Y, Tong J. Dynamic characteristics of dwarf Chinese hickory trees under impact excitations. International Journal of Agricultural and Biological Engineering, 2015, 8(1): 17–25.

20. He L, Zhou J F, Du X Q, Chen D, Zhang Q, Karkee M. Energy efficacy analysis of a mechanical shaker in sweet cherry harvesting. Biosystems Engineering, 2013, 116(4): 309–315.

21. Láng Z. A fruit tree stability model for static and dynamic loading. Biosystems Engineering, 2003, 85(4): 461–466.

22. Láng Z. Dynamic modelling structure of a fruit tree for inertial shaker system design. Biosystems Engineering, 2006, 93(1): 35–44.

23. Láng Z. A one degree of freedom damped fruit tree model. Transactions of the ASABE, 2008, 51(3): 823–829.

24. D'Agostino A, Giametta F, Giametta G, Mauro S, Zimbalatti G. Preliminary tests to assess the dynamics of the vibrations transmitted on olive trees by mechanized harvest by shakers. Acta Horticulturae, 2008, 791: 285–295.

25. Pezzi F, Caprara C. Mechanical grape harvesting: Investigation of the transmission of vibrations. Biosystems Engineering, 2009, 103(3): 281–286.

26. Castro-García S, Blanco-Roldán G L, Gil-Ribes J A, Agüera-Vega J. Dynamic analysis of olive trees in intensive orchards under forced vibration. Trees-Structure and Function,2008, 22(6): 795–802.

27. Wang Y C, Chen H T, Qiu L C. Modal experiment analysis on blackcurrant branches. Transactions of the CSAE, 2011, 27(Supp. 2): 45–49.

28. Rodriguez M, de Langre E, Moulia B. A scaling law for the effects of architecture and allometry on tree vibration modes suggests a biological tuning to modal compartmentalization. American Journal of Botany, 2008, 95(12): 1523–1537. https://doi.org/10.3732/ajb.0800161 PMID: 21628160

29. Rodriguez M, Ploquin S, Moulia B, de Langre E. The multimodal dynamics of a walnut tree: Experiments and Models. Journal of Applied Mechanics, 2012, 79(4): 1–5.

30. Moore J R, Maguire D A. Natural sway frequencies and damping ratios of trees: influence of crown structure. Trees-Structure and Function, 2005, 19 (4): 363–373.

31. Du X Q, Chen D, Zhang Q, Scharf P A, Whiting M D. Dynamic responses of sweet cherry trees under vibratory excitations. Biosystems Engineering, 2012, 111(3): 305–314.

32. Lin H, Xu L Y, Zhou H P, Xuan Y, Jia Z C, Chen Q. Relationship between frequency spectrum characteristics and vibration responses of *Ginkgo biloba* trees during mechanical harvesting operation. Transactions of the CSAE, 2017, 33(17): 51–57.

33. Salamon Z. Mechanical harvest of black currants and their sensitivity to damage. Acta Horticulturae,1993, 352: 109–112.